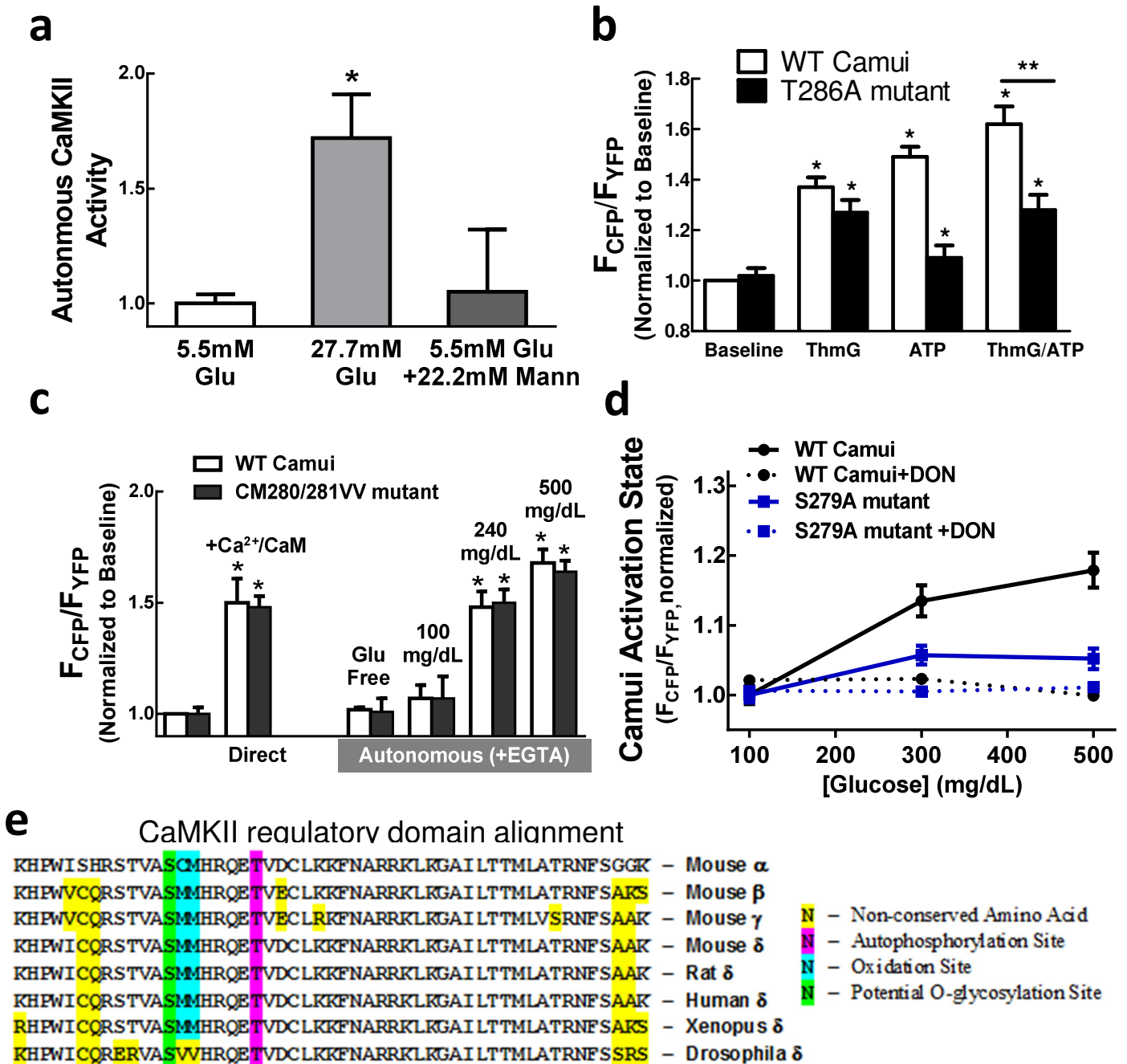
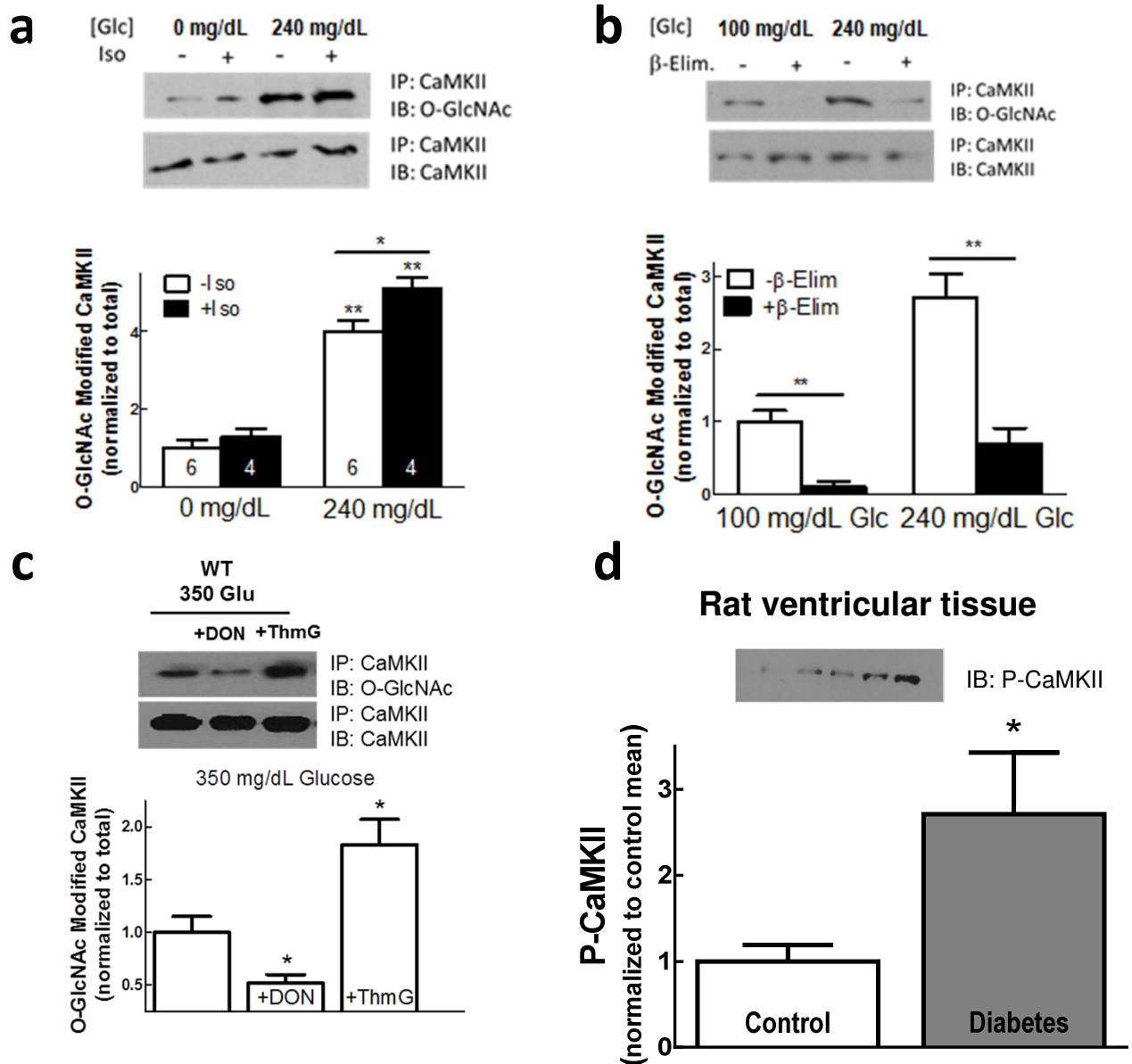


Supplemental Figure 1



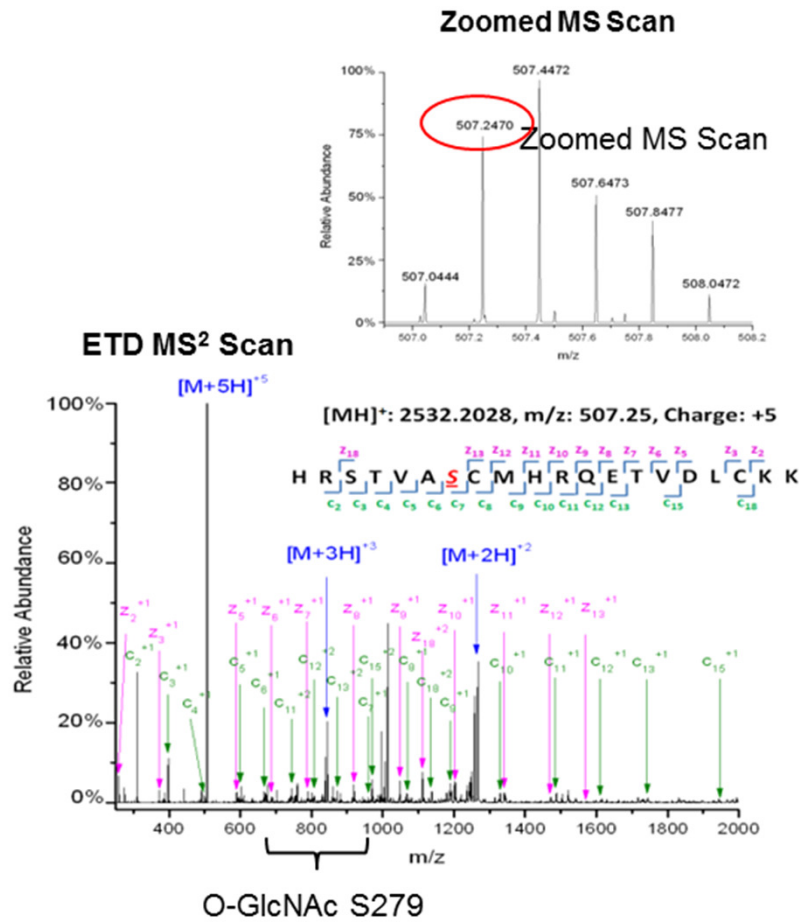
Supplemental Figure 1 - O-GlcNAc effect is not abolished by T286A or CM280/1VV mutation and CaMKII regulatory domain contains consensus O-GlcNAc modification sites. **a**, Increased [glucose], but not osmolarity matched [mannitol], activates CaMKII in HEK cells (n=9). **b**, O-GlcNAc dependent CaMKII activation is reduced but still present in T286A mutant Camui (n=9) **c**, Glucose dependent CaMKII activation is preserved in CM280/281VV mutant Camui expressed in HEK cell lysates (n=9). **d**, Activation of Camui by increased [glucose] is blunted in the S279A mutant and ablated entirely by DON. (n values: WT = 100, WT+DON = 72, S279A = 57, S279A+DON = 44 cells) **e**, These sites are conserved in all known isoforms of CaMKII and in a wide variety of mammalian species. Data are mean \pm s.e.m. * indicates p<0.05, ** indicates p<0.01 vs. control.

Supplemental Figure 2



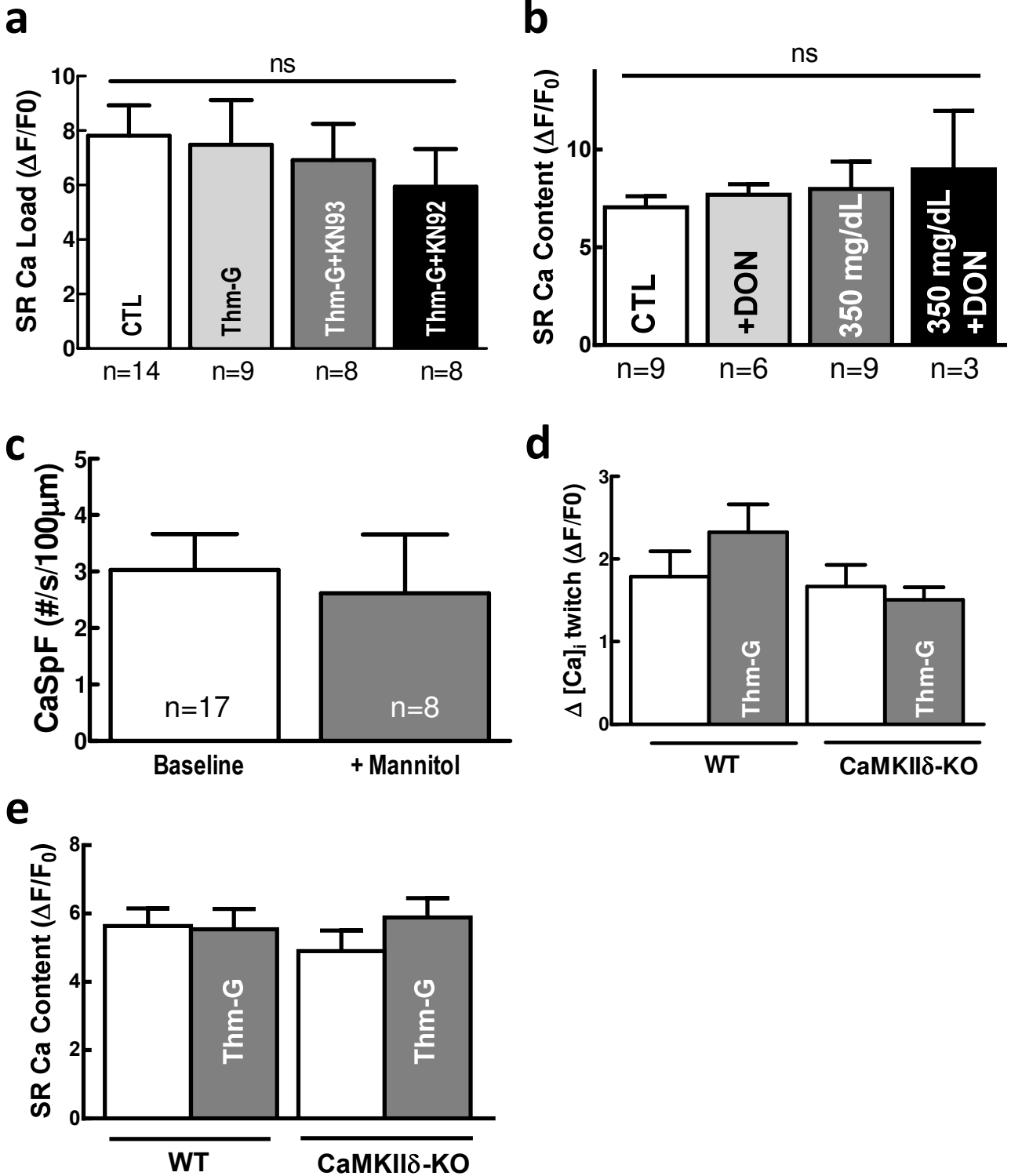
Supplemental Figure 2 - O-GlcNAc modification of CaMKII is enhanced in hyperglycemic conditions. **a**, Immunoblot with an O-GlcNAc specific antibody shows O-GlcNAc modification of CaMKII is inducible by increased glucose availability and is enhanced by Iso treatment. (n values indicated) **b**, O-GlcNAc modification of CaMKII is reversed by β -elimination reaction prior to immunoblot. **c**, O-GlcNAc modification of CaMKII is ablated by DON and enhanced by Thm-G. **d**, Autophosphorylation of cardiac CaMKII is significantly increased in a rat model of diabetes. n=3 for all immunoblots except where indicated. Data are mean \pm s.e.m. * indicates p<0.05, ** indicates p<0.01 vs. control.

Supplemental Figure 3



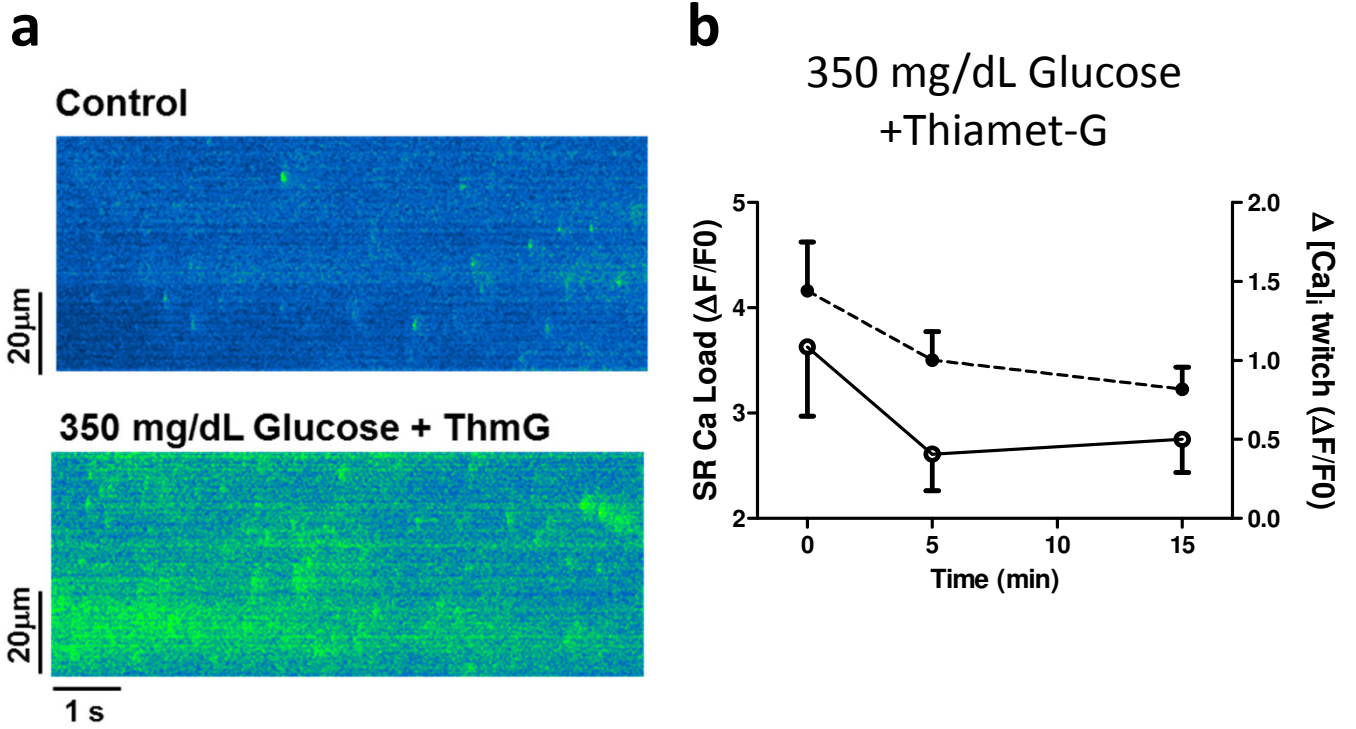
Supplemental Figure 3 – ETD-MS analysis confirms O-GlcNAc modification at S279A. A synthetic peptide encoding the regulatory domain of CaMKII was subjected to in vitro O-GlcNAc labeling followed by ETD-MS analysis. Examination of the 507.25 *m/z* peptide fragment (upper right inset) indicates the presence of an O-GlcNAc modification at S279 (*c6* to *c7* fragmentation).

Supplemental Figure 4



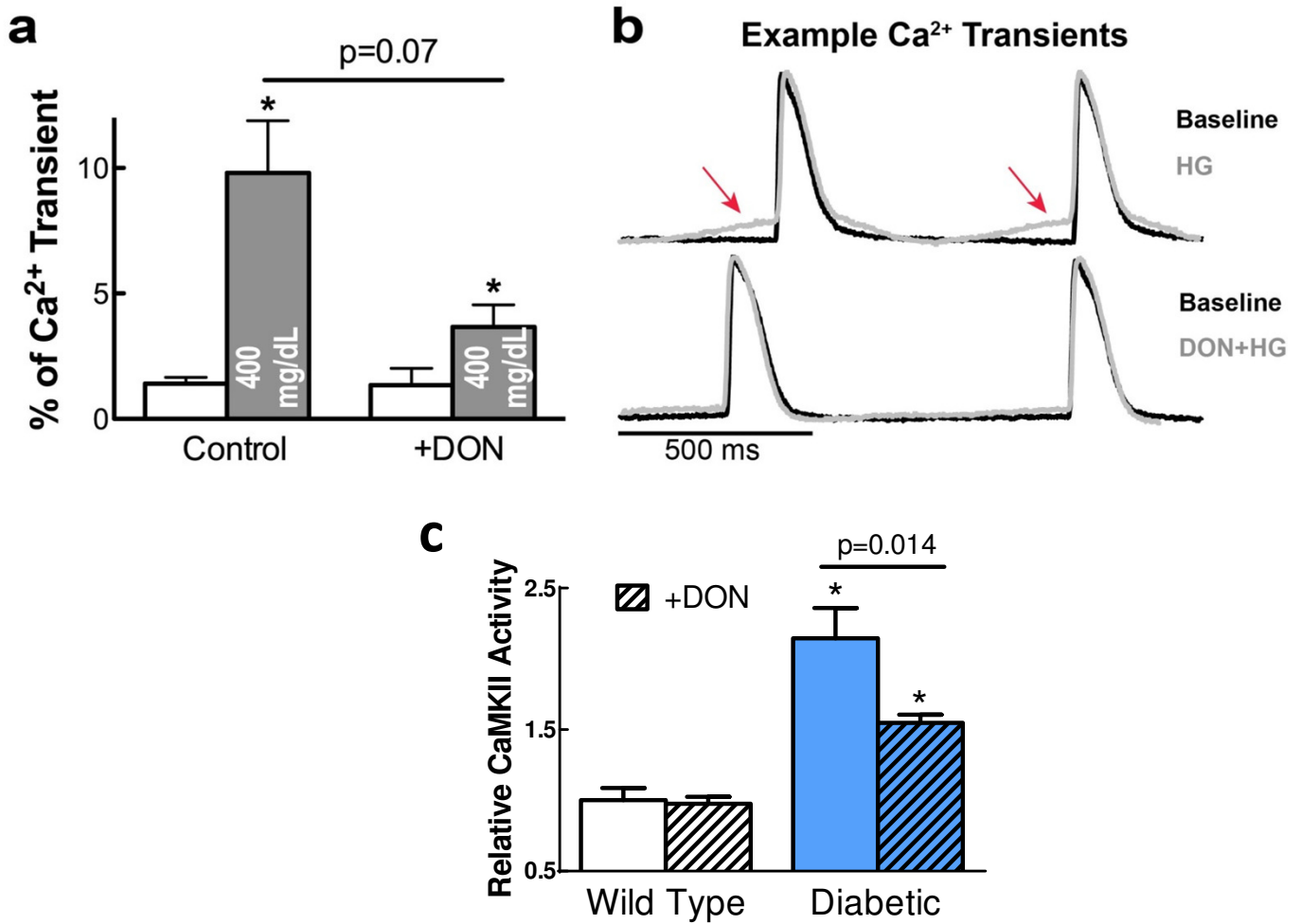
Supplemental Figure 4 - SR content is unaffected by Thm-G (a) or DON (b) in isolated rat myocytes (n values indicated). c, Mannitol does not enhance Ca²⁺ spark frequency in isolated rat myocytes. Ca²⁺ transient amplitude (d, n=13) and SR content (e, n=13) content are unaffected by Thm-G treatment in isolated myocytes from wild type (WT) or CaMKII δ knockout mice. Data are mean \pm s.e.m. ns indicates no significant difference.

Supplemental Figure 5



Supplemental Figure 5 - Simultaneous treatment with 350 mg/dL glucose and ThmG greatly enhances Ca^{2+} spark frequency **a**, and SR Ca^{2+} depletion **b**, in isolated rat myocytes ($n=6$). Data are mean \pm s.e.m.

Supplemental Figure 6



Supplemental Figure 6 - Diastolic $[Ca^{2+}]_i$ elevation under high glucose (HG) is suppressed by pre-treatment with 50 mM DON. **a**, Average diastolic Ca^{2+} elevation at baseline and following treatment with either HG or DON+HG. Ca^{2+} elevation was measured as the percent increase in the diastolic Ca^{2+} signal relative to the amplitude of the following Ca^{2+} transient. (n=3) **b**, Example Ca^{2+} transients during baseline conditions (black) and following treatment with either HG or DON+HG (gray). Minimal diastolic Ca^{2+} elevation occurs following pre-treatment with DON. n=3-4 rats for all data points. **c**, CaMKII activity is enhanced in heart lysate from diabetic rats (n=3), and this effect is blunted by treatment with DON. Data are mean \pm s.e.m. * indicates $p < 0.05$ vs. control.